



Identification of Acute Coronary Syndrome via Activation and Recovery Times in Body-Surface Mapping and Inverse Electrocardiography

Scott Marrus^{a,b}, Menghao Zhang^c, and Martin Arthur^{b,c}

^a Prairie Cardiovascular Consultants, Belleville, IL, USA

^b ATM Cardiac Diagnostics LLC, ST. Louis, MO USA

^c Electrical & Systems Engineering, School of Engineering, Washington University in St. Louis, USA

E-mail: rma@ese.wustl.edu

Abstract. Despite the central role of the traditional electrocardiogram (ECG) in the diagnosis of acute myocardial infarction (AMI), it is limited by both a lack of sensitivity and specificity, leading to a delay in diagnosis and consequently increased mortality, morbidity, readmission rates, and costs. Body surface electrical mapping and inverse electrocardiography provide more extensive and detailed electrical information than the 12-lead ECG, which could improve AMI diagnosis. Our Non-Invasive Cardiac Evaluation (NICE) system integrates body surface recordings with the mathematical reconstruction of heart-surface electrical potentials and uses signal analysis of both body surface and epicardial signals to identify subtle signs of ischemia or infarction. In preliminary studies on ten subjects, dispersion of ventricular activation seen on the body surface and dispersion of recovery seen on the heart surface separated troponin positive and negative patients with p values <0.01 . Differences between groups were not only statistically significant, but they were also sufficiently separated so that appropriate threshold values might be identified with useful positive and negative predictive values.

Keywords: Acute Myocardial Infarction; Body-Surface Maps; Heart-Torso Models; Inverse Electrocardiography

1. Introduction

Acute myocardial infarction (AMI), commonly referred to as heart attack, remains a leading cause of morbidity, mortality and healthcare expenditure in the United States, ranking as the fifth most expensive hospital diagnosis. Emergency departments in the United States receive 10 million annual visits for chest pain. Evaluation of these patients costs \$10-13 billion per year (Writing Group M, 2016). Unfortunately, despite the central role of the traditional electrocardiogram (ECG) in the diagnosis of AMI, the standard ECG remains limited by both a lack of sensitivity and specificity, leading to a delay in diagnosis and consequently increased mortality, morbidity, re-admission rates, and costs (Wang et al., 2009).

The cornerstone of acute MI management is rapid reperfusion therapy (either percutaneous coronary intervention (PCI) and stent placement or the administration of thrombolytic agents) to restore blood flow to the myocardium. Expedient reperfusion reduces acute MI mortality by 50% (Task Force on Practice G, 2013). The standard 12-lead ECG remains the foundation of rapid AMI diagnosis. Although the finding of ST elevations on the ECG is highly specific for a complete occlusion of a coronary vessel, (termed an ST-elevation MI, or STEMI), this group represents only 30% of all AMIs as seen in Fig. 1.

The remaining 70% of AMIs (termed non-ST-elevation MI, or NSTEMI) are diagnosed by an elevation in circulating cardiac biomarkers (typically cardiac-specific troponin) indicative of myocardial necrosis. There is, however, a delay of 3-6 hours after infarction before elevated troponin levels are detectable (Wang et al., 2009). It is also known that NSTEMIs encompass a spectrum of pathophysiology: ~15% are completely occluded vessels ("occult occlusions," accounting for ~25% of all total occlusions), ~40% have a sub-total occlusion, and ~45% do not have a coronary lesion amenable to intervention (Wang et al., 2009). Complete occlusions definitely warrant emergent treatment; the failure to promptly diagnose and treat 25% of complete occlusions results in ~6000 deaths/year in the US (our calculation). In addition to the improved care of occult occlusions, early diagnosis of sub-total occlusions will permit further studies of the benefit of prompt intervention in these patients [Amsterdam et al.2014].

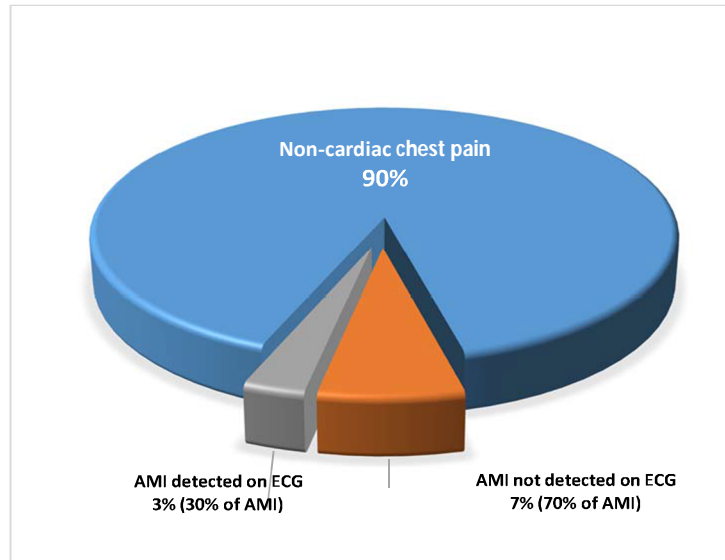


Figure 1: Although only 10% of patients with chest pain prove to have an acute MI (AMI), unfortunately, 70% of these AMIs are undiagnosed on the standard ECG.

Both high-resolution body surface electrical mapping and inverse electrocardiography provide more extensive and detailed electrical information than the 12-lead ECG and, in theory, could improve AMI diagnosis. Clinical application of these methods to AMI diagnosis, however, has been limited by the lack of an appropriate bioelectric metric for acute MI, which we address in this study.

2. Materials and Methods

The standard ECG is fundamentally limited by poor spatial sampling and by variations in individual torso anatomy. To improve spatial sampling, additional electrodes (typically 80 or more) can be used to provide a more complete sampling of the torso electrical signals, a method termed body surface potential mapping (Mirvis, 1987). To overcome the distorting effect of torso anatomy, patient-specific epicardial electrical potentials can be reconstructed based on body surface recordings in conjunction with a 3D model of cardiac and torso anatomy, a method termed electrocardiographic imaging (ECGI) or inverse electrocardiography (Beetner & Arthur, 1999, Ramanathan & Rudy, 2001, Rudy & Lindsay, 2015).

2.1 Inverse Electrocardiography Improves Detection of Myocardial Ischemia

Previous studies have demonstrated that inverse electrocardiography can accurately identify complete coronary occlusions (Macleod et al., 1995). To further explore the sensitivity of inverse solutions for sub-total occlusions (comprising 40% of NSTEMIs), raw data from experiments at the University of Utah were used (data obtained from the EDGAR database). Experiments were performed on an *ex vivo* canine heart suspended in a torso-shaped tank filled with electrolyte solution. Ischemia was introduced by a graded reduction in blood flow in the left anterior descending artery (LAD).

Using our inverse electrocardiographic methods, we found epicardial potentials from the recorded canine torso surface ECGs. We used singular value decomposition to quantify T wave complexity (a marker of ischemia (Al-Zaiti et al., 2015)). As shown in Fig. 2, the T wave complexity calculated from reconstructed epicardial potentials was $\sim 2 - 10x$ more sensitive to ischemia than the same metric calculated from body surface recordings, demonstrating that inverse electrocardiography can improve ischemia detection compared to the use of body surface recordings.

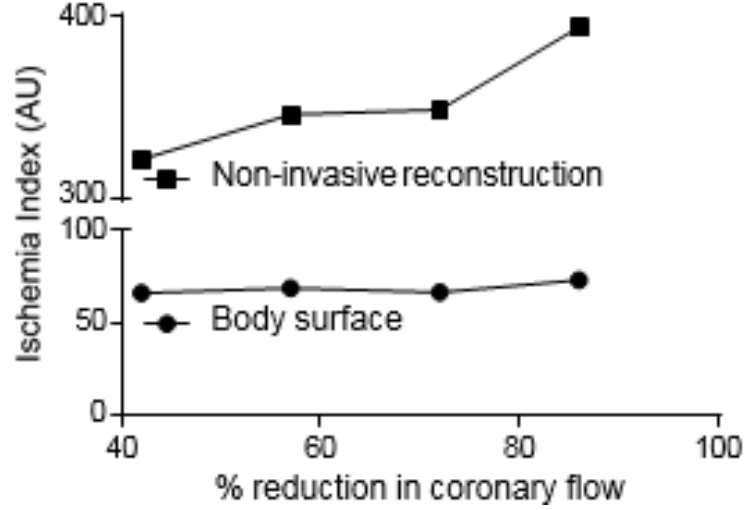


Figure 2: The ischemia index (based on T wave complexity) of reconstructed epicardial potentials (squares) is markedly more sensitive (p -value 0.038) to ischemia than body surface T wave complexity (p -value 0.490) (circles).

Inverse electrocardiography has been used to study arrhythmia substrates, activation patterns, and repolarization changes. It has also been used to guide invasive ablation procedures targeting PVCs, atrial tachycardia, and atrial fibrillation. It has, however, not been applied to the clinical diagnosis of ischemia and infarction.

2.2 Non-Invasive Cardiac Evaluation (NICE)

Our Non-Invasive Cardiac Evaluation (NICE) system for inverse electrocardiography integrates body surface recordings with a mathematical reconstruction of epicardial electrical potentials and uses signal analysis of both body surface and epicardial signals to identify subtle signs of ischemia or infarction.

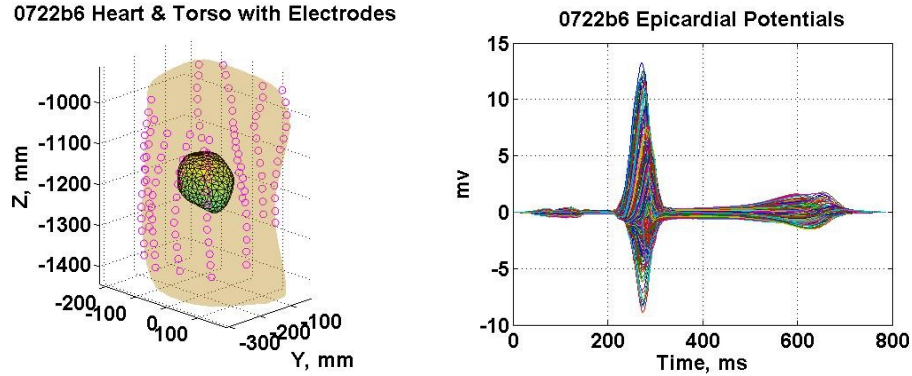


Figure 3: Left) Example of the torso and heart model with electrodes from CT scans. Right) Inverse solution on the heart surface in the model shown.

Our forward problem solution uses heart and torso geometry to find transfer coefficients \mathbf{Z}_{BH} that relate heart to body surface potentials (Ramsey et al., 1977).

$$\mathbf{Z}_{BH} = -(\mathbf{P}_{BB} - \mathbf{G}_{BH}\mathbf{G}_{HH}^{-1}\mathbf{P}_{HB})^{-1}(\mathbf{P}_{BH} - \mathbf{G}_{BH}\mathbf{G}_{HH}^{-1}\mathbf{P}_{HH}), \quad (1)$$

where \mathbf{P} is a matrix of solid angles and \mathbf{G} is a matrix of gradient integral coefficients. Transfer coefficients were calculated using 7-point Radon numerical integration to approximate gradient integral terms (Pilkington et al., 1987).

Conventional estimation of heart-surface potentials $\hat{\phi}_H$ using Tikhonov regularization from body-surface measurements $\hat{\phi}_B$ is given by

$$\hat{\phi}_H = (\mathbf{Z}_{BH}^* \mathbf{Z}_{BH} + \tau \mathbf{R}^* \mathbf{R})^{-1} \mathbf{Z}_{BH}^* \hat{\phi}_B \quad (2)$$

where \mathbf{Z}_{BH} are the transfer coefficients given in Eq. 1, τ is a regularization constant, and \mathbf{R} is a regularization matrix. $\mathbf{R} = \mathbf{I}$, the identity matrix, is known as zero-order Tikhonov regularization and is commonly used in the literature as a basis for comparison of regularization techniques.

Our NICE system comprises a) recording body surface signals from 120 electrodes b) construction of a 3D model of the torso and heart anatomy and c) inverse electrocardiography to reconstruct epicardial electrical signals. An example of model construction and the resulting inverse solution are shown in Fig. 3. The overall feasibility of the technique is demonstrated by the accurate reconstruction of the known pattern of electrical activation in the normal heart (Durrer et al., 1970), as shown in Fig. 4.

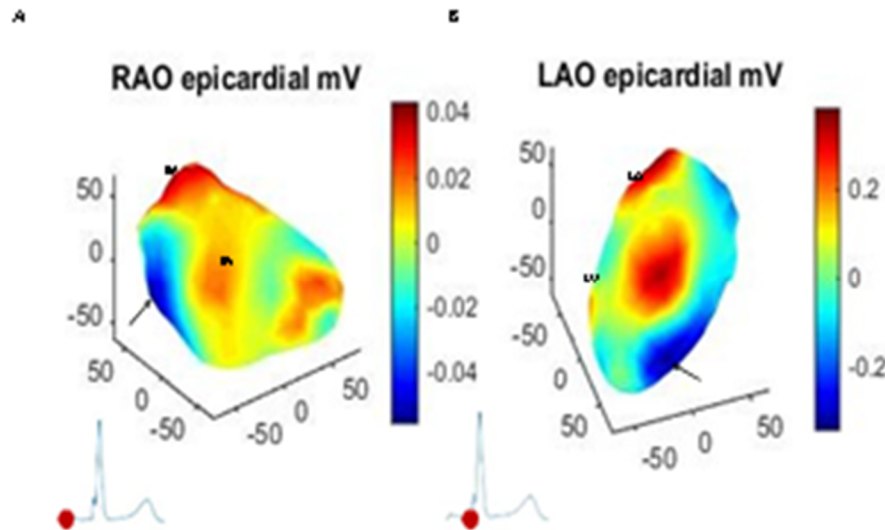


Figure 4: NICE accurately reconstructs normal cardiac electrical patterns. Local negative potentials reflect activation breakthrough to the epicardial surface. A. The site of the earliest atrial activation (arrow) occurs near the sinus node at the time of the body surface P wave onset (inset). B. The site of the earliest ventricular activation (arrow) occurs on the inferolateral LV wall at the onset of the body surface QRS (inset). Both locations are consistent with prior mapping studies. RA=right atrium, RV=right ventricle, LA=left atrium, LV=left ventricle, RAO=right anterior oblique view, LAO=left anterior oblique view.

Activation and recovery times on both body and epicardial surfaces were used as the metric to separate troponin positive from troponin negative subjects among those who presented with chest pain at our emergency department. Activation times were found from the minimum of the derivatives of electrograms on the heart and electrocardiograms on the body. Recovery times were found from the maximum of those derivatives.

Finite impulse response, linear-phase, Parks-McClellan-optimal-equiripple derivative operators were designed using tools available in Matlab™. Operator length was chosen to minimize noise due to differentiation while maximizing the accuracy of time estimates.

Fig. 5 shows a NICE estimation of activation time (AT), recovery time (RT) and the activation-recovery interval (ARI) in a normal male subject. Estimated times match expectations for a normal subject. Note the ARI map clearly delineates the atria from the ventricles.

2.3 Detection of Myocardial Infarction in Emergency Department Patients Using NICE

NICE was performed on ten subjects who presented to the Barnes-Jewish Hospital Emergency Department in St. Louis, MO, USA, with chest pain for a cardiac etiology. Both body surface recordings and the reconstructed epicardial potentials were analyzed. Patient-specific data were distilled into a score reflecting the probability of a heart attack. On clinical follow-up, five of the participants had abnormal troponin elevation, and five did not.

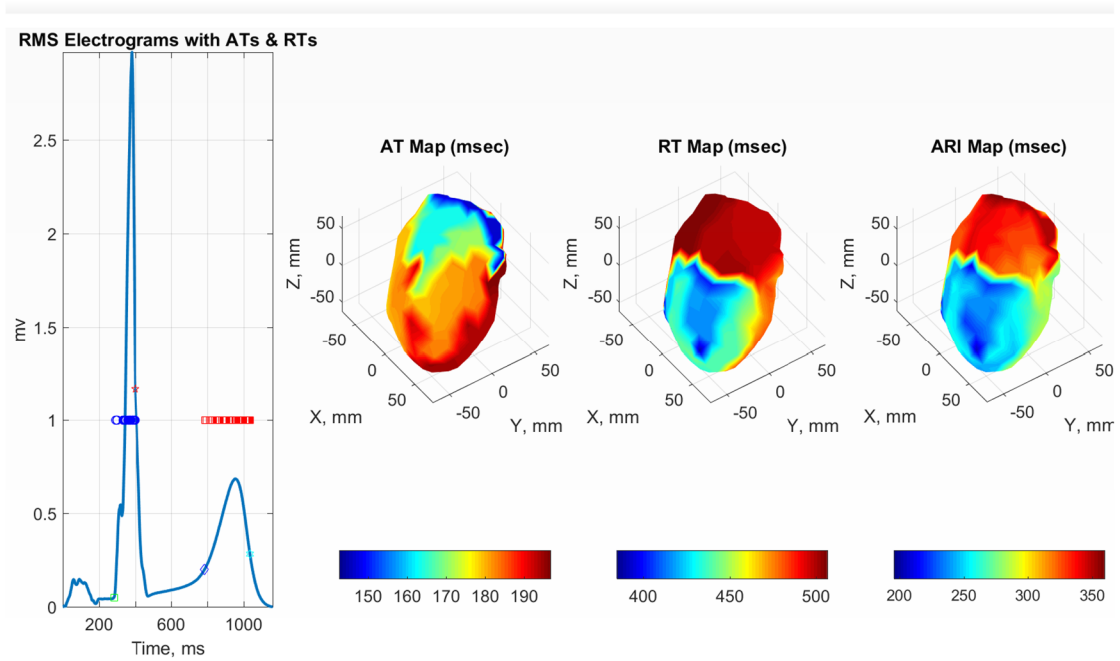


Figure 5: NICE estimation of activation time (AT), recovery time (RT) and the activation-recovery interval (ARI) in a normal male subject. Left) Activation (blue circles) and recovery (red squares) times on the root-mean-square value of inferred epicardial potentials with ATs in the QRS complex and RTs in the T wave. Left center) AT map, Right center) RT map and Right) ARI map. Estimated times match expectations for a normal subject. Note that the ARI map clearly delineates the atrial from the ventricles.

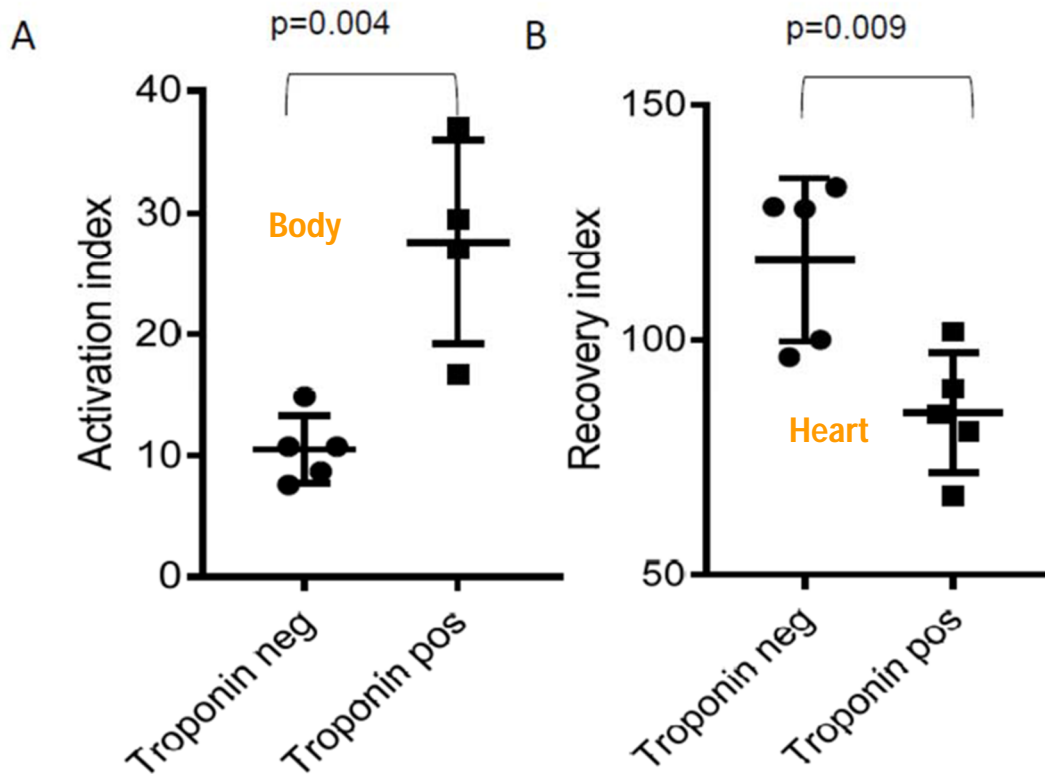


Figure 6: A. Patients with elevated troponin exhibit an increased dispersion of activation as measured on the body surface. B. Patients with elevated troponin also exhibit evidence of abnormal recovery as measured in reconstructed epicardial potentials. Both activation and recovery indices were significantly different ($p < 0.05$) when separated according to troponin assay results.

3. Results

Analysis of 10 subjects with NICE identified two promising metrics of acute MI (as defined by troponin elevation). The first, based on an analysis of body surface activation times and termed the "activation index," demonstrates a greater dispersion of activation time in subjects with elevated troponin (Fig. 6A), a finding likely corresponding to the known delay in activation in the context of myocardial ischemia (Akar & Akar, 2007). Notably, four of the five troponin-positive patients lacked a focal coronary lesion and, consistent with the predicted result, the dispersion of recovery ("recovery index") was significantly reduced in troponin-positive patients (Fig. 6B).

4. Discussion

Ischemia is known to affect the myocardial recovery by shortening the action potential (Akar & Akar, 2007). Depending on the spatial pattern of ischemia, this effect is predicted to either increase or decrease the dispersion of recovery. Localized transmural ischemia causing local action potential shortening is predicted to increase the dispersion of repolarization.

In contrast, global sub-endocardial ischemia, by shortening the sub-endocardial action potentials which are normally longer than mid-myocardial and sub-epicardial action potentials (Antzelevitch & Fish, 2001), is predicted to reduce the transmural dispersion of repolarization. Notably, four of the five troponin-positive patients lacked a focal coronary lesion and, consistent with the predicted result, the dispersion of recovery ("recovery index") was reduced in troponin-positive patients (Fig. 6B).

5. Conclusions

Our results demonstrate promising metrics which permit accurate discrimination between troponin positive and negative patients without the delay required for biomarker elevation. Importantly, the differences between groups are not only statistically significant but are also sufficiently separated that an appropriate threshold value can be identified which would provide useful positive and negative predictive values.

Acknowledgments

This work was supported by NIH grant R01 HL 50295, by AHA12FTF12040261 and by the Wilkinson Trust at Washington University in St. Louis, MO, USA.

References

- Akar, J. & Akar, F. (2007). Regulation of ion channels and arrhythmias in the ischemic heart. *J Electrocardiol*, 2007:S37–541.
- Al-Zaiti, S., Callaway, C., Kozik, T., Carey, M., & Pelter, M. (2015). Clinical utility of ventricular repolarization dispersion for real-time detection of non-ST elevation myocardial infarction in emergency departments. *J Am Heart Assoc*.
- Amsterdam, E., Wenger, N., Brindis, R., Casey, DE, J., Ganiats, T., Holmes, DR, J., Jaffe, A., Jneid, H., Kelly, R., Kontos, M., Levine, G., Liebson, P., Mukherjee, D., Peterson, E., Sabatine, M., Smalling, R., & Zieman, S. (2014). AHA/ACC guideline for the management of patients with non-st-elevation acute coronary syndromes: executive summary: a report of the American college of cardiology/American Heart Association task force on practice guidelines. *Circulation*, 130:2354–2394.
- Antzelevitch, C. & Fish, J. (2001). Electrical heterogeneity within the ventricular wall. *Basic Res Cardiol*, 96:517–527.
- Beetner, D. & Arthur, R. (1999). Direct inference of the spectra of pericardial potentials using the boundary-element method. *Annals of Biomed Engr*, 27(4):498–507.
- Durrer, D., van Dam, R., Freud, G., Janso, M., Meijler, F., & Arzbaecher, R. (1970). Total excitation of the isolated human heart. *Circulation*, 41:899–912.
- Macleod, R., Gardner, M., Miller, R., & Haracek, B. (1995). Application of an electrocardiographic inverse solution to localize ischemia during coronary angioplasty. *J Cardiovasc Electrophysiol*, 6:2–18.
- Mirvis, D. (1987). Current status of body surface electrocardiographic mapping. *Circulation*, 75(4):684–688.
- Pilkington, T., Morrow, M., & Stanley, P. (1987). A comparison of finite element and integral equation formulations for the calculation of electrocardiographic potentials - II. *IEEE Trans on Biomed Engr*, 34(3):258–260.
- Ramanathan, C. & Rudy, Y. (2001). Electrocardiographic imaging: II Effect of torso inhomogeneities on noninvasive reconstruction of epicardial potentials, electrograms, and isochrones. *J Cardiovasc Electrophysiol*, 12(2):241–252.
- Ramsey, M., Barr, R., & Spach, M. (1977). Comparison of measured torso potentials with those simulated from epicardial potentials for ventricular depolarization and repolarization in the intact dog. *Circulation Research*, 41:660–672.
- Rudy, Y. & Lindsay, B. (2015). Electrocardiographic imaging of heart rhythm disorders: from bench to bedside. *Card Electrophysiol Clin*, 7:17–35.
- Task Force on Practice G (2013). ACCF-AHA guideline for the management of st-elevation myocardial infarction. *Circulation*, 127:e362–425.
- Wang, T., Zhang, M., et al. (2009). Incidence, distribution, and prognostic impact of occluded culprit arteries among patients with non-st elevation acute coronary syndromes undergoing diagnostic angiography. *American Heart J*, 157:716–723.
- Writing Group M (2016). Heart disease and stroke statistics-2016 update: A report from the American heart association. *Circulation*, 133:e38–360.